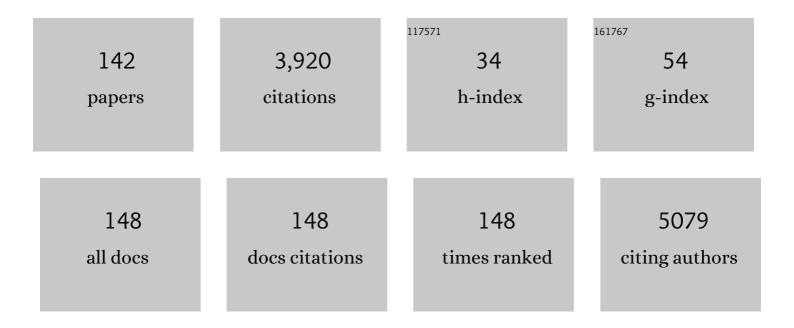
List of Publications by Year in descending order

Source: https://exaly.com/author-pdf/4610693/publications.pdf Version: 2024-02-01



#	Article	lF	CITATIONS
1	Suspendable macromolecules are responsible for ice nucleation activity of birch and conifer pollen. Atmospheric Chemistry and Physics, 2012, 12, 2541-2550.	1.9	251
2	Size-Dependent Optical Properties of MgO Nanocubes. Angewandte Chemie - International Edition, 2005, 44, 4917-4920.	7.2	205
3	Methane dry reforming over ceria-zirconia supported Ni catalysts. Catalysis Today, 2016, 277, 234-245.	2.2	196
4	Low temperature fullerene encapsulation in single wall carbon nanotubes: synthesis of N@C60@SWCNT. Chemical Physics Letters, 2004, 383, 362-367.	1.2	122
5	Cation diffusion in La0.6Sr0.4CoO3â^î´ below 800 °C and its relevance for Sr segregation. Physical Chemistry Chemical Physics, 2014, 16, 2715.	1.3	104
6	Stability and Photoelectronic Properties of Layered Titanate Nanostructures. Journal of the American Chemical Society, 2009, 131, 6198-6206.	6.6	101
7	Optical Surface Properties and Morphology of MgO and CaO Nanocrystals. Journal of Physical Chemistry B, 2006, 110, 13866-13871.	1.2	81
8	Dislocations Accelerate Oxygen Ion Diffusion in La _{0.8} Sr _{0.2} MnO ₃ Epitaxial Thin Films. ACS Nano, 2017, 11, 11475-11487.	7.3	80
9	Novel Optical Surface Properties of Ca2+-Doped MgO Nanocrystals. Nano Letters, 2005, 5, 1889-1893.	4.5	69
10	Chemical Control of Photoexcited States in Titanate Nanostructures. Nano Letters, 2007, 7, 433-438.	4.5	65
11	Factors Influencing Hydride Formation in a Pd/TiO2 Catalyst. Journal of Physical Chemistry B, 2006, 110, 17090-17095.	1.2	61
12	Extracellular bone matrix exhibits hardening elastoplasticity and more than double cortical strength: Evidence from homogeneous compression of non-tapered single micron-sized pillars welded to a rigid substrate. Journal of the Mechanical Behavior of Biomedical Materials, 2015, 52, 51-62.	1.5	60
13	Transmission electron microscope characterization of cast and hotâ€workedRâ€Feâ€B:Cu(R=Nd,Pr) permanent magnets. Journal of Applied Physics, 1991, 70, 6456-6458.	1.1	57
14	In Situ-Determined Catalytically Active State of LaNiO ₃ in Methane Dry Reforming. ACS Catalysis, 2020, 10, 1102-1112.	5.5	55
15	Solar Light and Dopant-Induced Recombination Effects: Photoactive Nitrogen in TiO ₂ as a Case Study. Journal of Physical Chemistry C, 2010, 114, 18067-18072.	1.5	54
16	Particles Coming Together:  Electron Centers in Adjoined TiO2 Nanocrystals. Journal of Physical Chemistry B, 2006, 110, 7605-7608.	1.2	52
17	Microstructure and Mechanical Properties of HVOF Sprayed Nanocrystalline Cr ₃ C ₂ -25(Ni20Cr) Coating. Journal of Thermal Spray Technology, 2006, 15, 372-381.	1.6	51
18	Solidâ^'Solid Interface Formation in TiO2Nanoparticle Networks. Langmuir, 2011, 27, 1946-1953.	1.6	49

2

#	Article	IF	CITATIONS
19	Preparation and TEM-study of sintered Nd/sub 18/Fe/sub 74/B/sub 6/Ga/sub 1/Nb/sub 1/ magnets. IEEE Transactions on Magnetics, 1993, 29, 2773-2775.	1.2	48
20	Surface modification processes during methane decomposition on Cu-promoted Ni–ZrO ₂ catalysts. Catalysis Science and Technology, 2015, 5, 967-978.	2.1	48
21	Surface composition changes of CuNi-ZrO2 during methane decomposition: An operando NAP-XPS and density functional study. Catalysis Today, 2017, 283, 134-143.	2.2	48
22	Fullerene release from the inside of carbon nanotubes: A possible route toward drug delivery. Chemical Physics Letters, 2007, 445, 288-292.	1.2	47
23	Understanding electrochemical switchability of perovskite-type exsolution catalysts. Nature Communications, 2020, 11, 4801.	5.8	46
24	Charge Separation in Layered Titanate Nanostructures: Effect of Ion Exchange Induced Morphology Transformation. Angewandte Chemie - International Edition, 2008, 47, 1496-1499.	7.2	43
25	Preparation, magnetic properties and microstructure of lean rare-earth permanent magnetic materials. Journal of Magnetism and Magnetic Materials, 2000, 219, 186-198.	1.0	42
26	Chemistry and morphology of driedâ€up pollen suspension residues. Journal of Raman Spectroscopy, 2013, 44, 1654-1658.	1.2	42
27	Microwave-assisted solution–liquid–solid growth of Ge _{1â^'x} Sn _x nanowires with high tin content. Chemical Communications, 2015, 51, 12282-12285.	2.2	42
28	Imaging of low temperature induced SMSI on Pd/TiO2 catalysts. Catalysis Letters, 2007, 114, 91-95.	1.4	41
29	Microstresses and crack formation in AlSi7MgCu and AlSi17Cu4 alloys for engine components. Acta Materialia, 2014, 81, 401-408.	3.8	40
30	Functional Interfaces in Pure and Blended Oxide Nanoparticle Networks: Recombination versus Separation of Photogenerated Charges. Journal of Physical Chemistry C, 2009, 113, 15792-15795.	1.5	39
31	Microwave-Assisted Ge _{1–<i>x</i>} Sn _{<i>x</i>} Nanowire Synthesis: Precursor Species and Growth Regimes. Chemistry of Materials, 2015, 27, 6125-6130.	3.2	39
32	Accelerated mechanical fatigue testing and lifetime of interconnects in microelectronics. Procedia Engineering, 2010, 2, 511-519.	1.2	38
33	Steering the Methane Dry Reforming Reactivity of Ni/La ₂ O ₃ Catalysts by Controlled In Situ Decomposition of Doped La ₂ NiO ₄ Precursor Structures. ACS Catalysis, 2021, 11, 43-59.	5.5	38
34	Preparation and transmission electron microscope investigation of sintered Nd15.4Fe75.7B6.7Cu1.3Nb0.9magnets. Journal of Applied Physics, 1994, 76, 6241-6243.	1.1	36
35	Porphyrin Metalation at MgO Surfaces: A Spectroscopic and Quantum Mechanical Study on Complementary Model Systems. Chemistry - A European Journal, 2016, 22, 1744-1749.	1.7	36
36	Irreversible degradation of Nb ₃ Sn Rutherford cables due to transverse compressive stress at room temperature. Superconductor Science and Technology, 2018, 31, 065009.	1.8	35

JOHANNES BERNARDI

#	Article	IF	CITATIONS
37	The CERN FCC Conductor Development Program: A Worldwide Effort for the Future Generation of High-Field Magnets. IEEE Transactions on Applied Superconductivity, 2019, 29, 1-9.	1.1	35
38	Encapsulating C59N azafullerene derivatives inside single-wall carbon nanotubes. Carbon, 2006, 44, 1958-1962.	5.4	34
39	Epitaxial Ge _{0.81} Sn _{0.19} Nanowires for Nanoscale Mid-Infrared Emitters. ACS Nano, 2019, 13, 8047-8054.	7.3	34
40	Pushing the Composition Limit of Anisotropic Ge _{1–<i>x</i>} Sn _{<i>x</i>} Nanostructures and Determination of Their Thermal Stability. Chemistry of Materials, 2017, 29, 9802-9813.	3.2	33
41	Zinc oxide scaffolds on MgO nanocubes. Nanotechnology, 2010, 21, 355603.	1.3	31
42	Visualizing catalyst heterogeneity by a Âmultifrequential oscillating reaction. Nature Communications, 2018, 9, 600.	5.8	31
43	Lorentz microscopy of giant magnetoresistive AuCo alloys. Physica Status Solidi A, 1995, 150, 171-184.	1.7	30
44	Trapping of photogenerated charges in oxide nanoparticles. Materials Science and Engineering C, 2005, 25, 664-668.	3.8	30
45	Diffusion parameters of grain-growth inhibitors in WC based hardmetals with Co, Fe/Ni and Fe/Co/Ni binder alloys. International Journal of Refractory Metals and Hard Materials, 2015, 49, 67-74.	1.7	30
46	Porphyrin Metalation at the MgO Nanocube/Toluene Interface. ACS Applied Materials & Interfaces, 2015, 7, 22962-22969.	4.0	30
47	Microstructural influence on magnetic properties and giant magnetoresistance of melt-spun gold-cobalt. Scripta Metallurgica Et Materialia, 1995, 33, 1647-1666.	1.0	28
48	Photoluminescent Nanoparticle Surfaces: The Potential of Alkaline Earth Oxides for Optical Applications. Advanced Materials, 2008, 20, 4840-4844.	11.1	28
49	Electrochemical properties of La0.6Sr0.4CoO3â^îŕ thin films investigated by complementary impedance spectroscopy and isotope exchange depth profiling. Solid State Ionics, 2014, 256, 38-44.	1.3	28
50	Phase Separation at the Nanoscale: Structural Properties of BaO Segregates on MgO-Based Nanoparticles. Journal of Physical Chemistry C, 2011, 115, 15853-15861.	1.5	26
51	Operando XAS and NAP-XPS investigation of CO oxidation on meso- and nanoscale CoO catalysts. Catalysis Today, 2019, 336, 139-147.	2.2	25
52	A Comparative Discussion of the Catalytic Activity and CO2-Selectivity of Cu-Zr and Pd-Zr (Intermetallic) Compounds in Methanol Steam Reforming. Catalysts, 2017, 7, 53.	1.6	24
53	A New Preparation Pathway to Well-Defined In2O3Nanoparticles at Low Substrate Temperatures. Journal of Physical Chemistry C, 2008, 112, 918-925.	1.5	23
54	Microstructural Investigation of Interfacial Features in Al Wire Bonds. Journal of Electronic Materials, 2012, 41, 3436-3446.	1.0	22

#	Article	IF	CITATIONS
55	Resolving multifrequential oscillations and nanoscale interfacet communication in single-particle catalysis. Science, 2021, 372, 1314-1318.	6.0	22
56	Elasto-plastic deformation in Al-Cu cast alloys for engine components. Journal of Alloys and Compounds, 2019, 775, 617-627.	2.8	21
57	Colloidally Prepared Pt Nanowires versus Impregnated Pt Nanoparticles: Comparison of Adsorption and Reaction Properties. Langmuir, 2010, 26, 16330-16338.	1.6	20
58	Synthesis and thermal behavior of tin-based alloy (Sn–Ag–Cu) nanoparticles. Nanoscale, 2015, 7, 5843-5851.	2.8	20
59	Adsorption, Ordering, and Metalation of Porphyrins on MgO Nanocube Surfaces: The Directional Role of Carboxylic Anchoring Groups. Journal of Physical Chemistry C, 2016, 120, 26879-26888.	1.5	20
60	Magnetic and microstructural properties of sintered FeNdB-based magnets with Ga and Nb additions. Journal of Magnetism and Magnetic Materials, 1994, 138, 294-300.	1.0	19
61	Permanent magnets — New microstructural aspects. Scripta Metallurgica Et Materialia, 1995, 33, 1781-1791.	1.0	19
62	Tribological behaviour of Ti containing nanocomposite DLC films under milli-Newton load range. Diamond and Related Materials, 2008, 17, 2010-2018.	1.8	19
63	Microstructural and Chemical Evolution and Analysis of a Self-Activating CO ₂ -Selective Cu–Zr Bimetallic Methanol Steam Reforming Catalyst. Journal of Physical Chemistry C, 2016, 120, 25395-25404.	1.5	19
64	Changing interfaces: Photoluminescent ZnO nanoparticle powders in different aqueous environments. Surface Science, 2016, 652, 253-260.	0.8	19
65	Hydroxylation Induced Alignment of Metal Oxide Nanocubes. Angewandte Chemie - International Edition, 2017, 56, 1407-1410.	7.2	19
66	Hydrogen Oxidation on Stepped Rh Surfaces: µm-Scale versus Nanoscale. Catalysis Letters, 2016, 146, 1867-1874.	1.4	18
67	Thin water films and particle morphology evolution in nanocrystalline MgO. Journal of the American Ceramic Society, 2018, 101, 4994-5003.	1.9	18
68	Crystallographic and electronic evolution of lanthanum strontium ferrite (La _{0.6} Sr _{0.4} FeO _{3â~î^}) thin film and bulk model systems during iron exsolution. Physical Chemistry Chemical Physics, 2019, 21, 3781-3794.	1.3	18
69	Surface-Structure Libraries: Multifrequential Oscillations in Catalytic Hydrogen Oxidation on Rhodium. Journal of Physical Chemistry C, 2019, 123, 4217-4227.	1.5	18
70	The effect of V or W additives to microstructure and coercivity of Nd-Fe-B based magnets. IEEE Transactions on Magnetics, 1992, 28, 2127-2129.	1.2	17
71	BaO Clusters on MgO Nanocubes: A Quantitative Analysis of Opticalâ€Powder Properties. Small, 2010, 6, 582-588.	5.2	17
72	Growth of monocrystalline In2O3 nanowires by a seed orientation dependent vapour–solid–solid mechanism. Journal of Materials Chemistry C, 2014, 2, 5747.	2.7	17

#	Article	IF	CITATIONS
73	Surface-specific visible light luminescence from composite metal oxide nanocrystals. Journal of Materials Science, 2015, 50, 8153-8165.	1.7	17
74	Role of the heating rate up to the annealing temperature on the hysteretic properties of hard magnetic materials prepared from amorphous precursors. Journal of Alloys and Compounds, 1993, 191, 127-130.	2.8	16
75	Nanoparticles as a Support: CaO Deposits on MgO Cubes. Journal of Physical Chemistry C, 2008, 112, 9120-9123.	1.5	16
76	Surface Spectroscopy on UHV-Grown and Technological Ni–ZrO2 Reforming Catalysts: From UHV to Operando Conditions. Topics in Catalysis, 2016, 59, 1614-1627.	1.3	16
77	Boosting Hydrogen Production from Methanol and Water by inâ€situ Activation of Bimetallic Cuâ^'Zr Species. ChemCatChem, 2016, 8, 1778-1781.	1.8	16
78	Setting Directions: Anisotropy in Hierarchically Organized Porous Silica. Chemistry of Materials, 2017, 29, 7969-7975.	3.2	16
79	A novel magnetic microfluidic platform for on-chip separation of 3 types of silica coated magnetic nanoparticles (Fe3O4@SiO2). Sensors and Actuators A: Physical, 2018, 270, 223-230.	2.0	16
80	Mechanistic in situ insights into the formation, structural and catalytic aspects of the La2NiO4 intermediate phase in the dry reforming of methane over Ni-based perovskite catalysts. Applied Catalysis A: General, 2021, 612, 117984.	2.2	16
81	One-Step Flame Synthesis of Ultrafine SiO2â^'C Nanocomposite Particles with High Carbon Loading and Their Carbothermal Conversion. Industrial & Engineering Chemistry Research, 2007, 46, 4273-4281.	1.8	15
82	Outstanding Oxygen Reduction Kinetics of La _{0.6} Sr _{0.4} FeO _{3â^´l´} Surfaces Decorated with Platinum Nanoparticles. Journal of the Electrochemical Society, 2020, 167, 104514.	1.3	15
83	When Fewer Photons Do More: A Comparative O ₂ Photoadsorption Study on Vapor-Deposited TiO ₂ and ZrO ₂ Nanocrystal Ensembles. Journal of Physical Chemistry C, 2009, 113, 9175-9181.	1.5	14
84	Critical current anisotropy of GdBCO tapes grown on ISD–MgO buffered substrate. Superconductor Science and Technology, 2015, 28, 124002.	1.8	14
85	Synthesis of nanowires in room temperature ambient: A focused ion beam approach. Applied Physics Letters, 2006, 88, 163114.	1.5	13
86	An attempt to synthesize Sn-Zn-Cu alloy nanoparticles. Materials Letters, 2016, 178, 10-14.	1.3	13
87	A Combined TEM/STEM and Micromagnetic Study of the Anisotropic Nature of Grain Boundaries and Coercivity in Nd-Fe-B Magnets. Advances in Materials Science and Engineering, 2017, 2017, 1-12.	1.0	13
88	Carbon aerogels with improved flexibility by sphere templating. RSC Advances, 2018, 8, 27326-27331.	1.7	13
89	Steering the methanol steam reforming performance of Cu/ZrO2 catalysts by modification of the Cu-ZrO2 interface dimensions resulting from Cu loading variation. Applied Catalysis A: General, 2021, 623, 118279.	2.2	13
90	Electron microscopy of giant magnetoresistive granular Auî—,Co alloys. Journal of Magnetism and Magnetic Materials, 1996, 157-158, 153-155.	1.0	12

#	Article	IF	CITATIONS
91	Photoexcitation of Local Surface Structures on Strontium Oxide Grains. Journal of Physical Chemistry C, 2007, 111, 8069-8074.	1.5	12
92	Pt–B System Revisited: Pt ₂ B, a New Structure Type of Binary Borides. Ternary WAl ₁₂ -Type Derivative Borides. Inorganic Chemistry, 2015, 54, 10958-10965.	1.9	12
93	Complex oxide thin films: Pyrochlore, defect fluorite and perovskite model systems for structural, spectroscopic and catalytic studies. Applied Surface Science, 2018, 452, 190-200.	3.1	12
94	Conductive AFM and chemical analysis of highly conductive paths in DC degraded PZT with Ag/Pd electrodes. Solid State Ionics, 2013, 244, 5-16.	1.3	11
95	Spores of many common airborne fungi reveal no ice nucleation activity in oil immersion freezing experiments. Biogeosciences, 2013, 10, 8083-8091.	1.3	11
96	Diallyl disulphide as natural organosulphur friction modifier via the in-situ tribo-chemical formation of tungsten disulphide. Applied Surface Science, 2018, 428, 659-668.	3.1	11
97	Effects of inhomogeneities on pinning force scaling in Nb ₃ Sn wires. Superconductor Science and Technology, 2018, 31, 084002.	1.8	11
98	Stability and Local Environment of Iron in Vapor Phase Grown MgO Nanocrystals. Journal of Physical Chemistry C, 2017, 121, 24292-24301.	1.5	10
99	Iron Precursor Decomposition in the Magnesium Combustion Flame: A New Approach for the Synthesis of Particulate Metal Oxide Nanocomposites. Particle and Particle Systems Characterization, 2017, 34, 1700109.	1.2	10
100	Evolution of the superconducting properties from binary to ternary APC-Nb ₃ Sn wires. Superconductor Science and Technology, 2021, 34, 035028.	1.8	10
101	TEM Investigation of Multilayered Structures in Heterogeneous AuCo Alloys. Physica Status Solidi A, 1995, 147, 165-175.	1.7	9
102	The nano heat effect of replacing macro-particles by nano-particles in drop calorimetry: the case of core/shell metal/oxide nano-particles. RSC Advances, 2018, 8, 8856-8869.	1.7	9
103	Redox mechanism in the NiP2 electrode for Li-ion batteries: A DFT study coupled with local chemical bond analyses. Ionics, 2008, 14, 197-202.	1.2	8
104	Role of Impurities and PSBs on Microcracking of Polycrystalline Copper at Very High Numbers of Cycles. Key Engineering Materials, 0, 465, 29-34.	0.4	8
105	Synthesis and characterisation of (Fe,Co)2–3B microcrystalline alloys. Journal of Alloys and Compounds, 2015, 644, 199-204.	2.8	8
106	Sn-Ag-Cu Nanosolders: Solder Joints Integrity and Strength. Journal of Electronic Materials, 2016, 45, 4390-4399.	1.0	8
107	Mechanism of Rare Earth Incorporation and Crystal Growth of Rare Earth Containing Type-I Clathrates. Crystal Growth and Design, 2016, 16, 25-33.	1.4	8
108	Assessing composition gradients in multifilamentary superconductors by means of magnetometry methods. Superconductor Science and Technology, 2017, 30, 014011.	1.8	8

#	Article	IF	CITATIONS
109	Cobalt and Iron Ions in MgO Nanocrystals: Should They Stay or Should They Go. Journal of Physical Chemistry C, 2019, 123, 25991-26004.	1.5	8
110	Encapsulating C59N azafullerenes inside single-wall carbon nanotubes. Physica Status Solidi (B): Basic Research, 2006, 243, 3263-3267.	0.7	7
111	Who Does the Job? How Copper Can Replace Noble Metals in Sustainable Catalysis by the Formation of Copper–Mixed Oxide Interfaces. ACS Catalysis, 2022, 12, 7696-7708.	5.5	7
112	Magnetic and microstructural properties of FeNdB type magnets with additives. Journal of Magnetism and Magnetic Materials, 1995, 140-144, 1059-1060.	1.0	6
113	Toward Synthesis and Characterization of Unconventional C ₆₆ and C ₆₈ Fullerenes inside Carbon Nanotubes. Journal of Physical Chemistry C, 2014, 118, 30260-30268.	1.5	6
114	Cross-sectional nanoindentation (CSN) studies on the effect of thickness on adhesion strength of thin films. Journal Physics D: Applied Physics, 2015, 48, 035301.	1.3	6
115	Lead-supported germanium nanowire growth. Materials Letters, 2016, 173, 248-251.	1.3	6
116	Structural and Catalytic Properties of Ag- and Co ₃ O ₄ -Impregnated Strontium Titanium Ferrite SrTi _{0.7} Fe _{0.3} O _{3â~δ} in Methanol Steam Reforming. Industrial & Engineering Chemistry Research, 2017, 56, 13654-13662.	1.8	6
117	Impurity Segregation and Nanoparticle Reorganization of Indium Doped MgO Cubes. ChemNanoMat, 2019, 5, 634-641.	1.5	6
118	Performance modulation through selective, homogenous surface doping of lanthanum strontium ferrite electrodes revealed by <i>in situ</i> PLD impedance measurements. Journal of Materials Chemistry A, 2022, 10, 2973-2986.	5.2	6
119	Elucidating the role of earth alkaline doping in perovskite-based methane dry reforming catalysts. Catalysis Science and Technology, 2022, 12, 1229-1244.	2.1	6
120	Magnetic granularity in PLD-grown Fe(Se,Te) films on simple RABiTS templates. Superconductor Science and Technology, 2022, 35, 074001.	1.8	6
121	Analytical electron microscopy of Sm(Co,Fe,Cu, Zr)/sub 9/. IEEE Transactions on Magnetics, 1990, 26, 1385-1387.	1.2	5
122	Development of anin vitromodel on cellular adhesion on granular natural bone mineral under dynamic seeding conditions-A pilot study. Journal of Biomedical Materials Research - Part B Applied Biomaterials, 2009, 91B, 766-771.	1.6	5
123	Straightforward Solvothermal Synthesis toward Phase Pure Li ₂ CoPO ₄ F. Crystal Growth and Design, 2016, 16, 4999-5005.	1.4	5
124	Monolithic porous magnesium silicide. Dalton Transactions, 2017, 46, 8855-8860.	1.6	5
125	Influence of Local Inhomogeneities in the REBCO Layer on the Mechanism of Quench Onset in 2G HTS Tapes. IEEE Transactions on Applied Superconductivity, 2022, 32, 1-7.	1.1	5
126	Electronic Reducibility Scales with Intergranular Interface Area in Consolidated In ₂ O ₃ Nanoparticles Powders. Journal of Physical Chemistry C, 2016, 120, 4581-4588.	1.5	4

#	Article	IF	CITATIONS
127	Dependences of phase stability and thermoelectric properties of type-I clathrate Ba8Cu4.5Si6Ge35.5 on synthesis process parameters. Journal of Alloys and Compounds, 2017, 725, 783-791.	2.8	4
128	Heterogeneous Strain Distribution and Saturation of Geometrically Necessary Dislocations in a Ferritic–Pearlitic Steel during Lubricated Sliding. Advanced Engineering Materials, 2018, 20, 1700810.	1.6	4
129	Nanostructured clathrates and clathrateâ€based nanocomposites. Physica Status Solidi (A) Applications and Materials Science, 2016, 213, 784-801.	0.8	3
130	Formation of Pd-Ce intermetallic compounds by reductive metal-support interaction. Journal of Solid State Chemistry, 2018, 265, 176-183.	1.4	3
131	From sol–gel prepared porous silica to monolithic porous Mg2Si/MgO composite materials. Journal of Sol-Gel Science and Technology, 2019, 89, 295-302.	1.1	3
132	Observation and characterization of a twinned monoclinic phase as a product of the solid state decomposition of Nd2Fe14B. Journal of Materials Research, 1992, 7, 1762-1768.	1.2	2
133	Structural and Chemical Investigations of (La, Sr)CoO _{3-Î′} Thin Film Electrodes Exhibiting Very Fast Oxygen Reduction Kinetics. ECS Transactions, 2009, 25, 2397-2402.	0.3	2
134	Elasto-plastic deformation within diamond reinforced metals for thermal management. Diamond and Related Materials, 2016, 70, 52-58.	1.8	2
135	Microbeam bending of hydrated human cortical bone lamellae from the central region of the body of femur shows viscoelastic behaviour. Journal of the Mechanical Behavior of Biomedical Materials, 2022, 125, 104815.	1.5	2
136	Characterization of Frictional Stressed White Etching Layers out of Cutting Tools by Means of Transmission Electron Microscopy (TEM). Praktische Metallographie/Practical Metallography, 2014, 51, 485-498.	0.1	2
137	Ionic bis-nanoparticle networks. Monatshefte Für Chemie, 2012, 143, 519-525.	0.9	1
138	Influence of experimental constraints on micromechanical assessment of micromachined hard-tissue samples. Journal of the Mechanical Behavior of Biomedical Materials, 2020, 106, 103741.	1.5	1
139	Nb ₃ Sn Wires for the Future Circular Collider at CERN: Microstructural Investigation of Different Wire Layouts. IEEE Transactions on Applied Superconductivity, 2021, 31, 1-5.	1.1	1
140	Surface crack propagation and morphology in cutting tools. Industrial Lubrication and Tribology, 2016, 68, 141-148.	0.6	0
141	Organisation von Metalloxidâ€Nanowürfeln durch Hydroxylierung. Angewandte Chemie, 2017, 129, 1428-1432.	1.6	0
142	USTEM – TRANSMISSIONSELEKTRONENMIKROSKOPIE AUF HÖCHSTEM / NIVEAU USTEM – TRANSMISSION ELECTRON MICROSCOPY AT THE HIGHEST LEVEL. , 2016, , 89-94.		0